



Fluorescent Polymeric Sensor for Selective and Sensitive Detection of Cu(II) Ions in Aqueous Medium

Soner Çubuk^{*1} , Nur Koçoğlu¹ , Gülay Bayramoğlu² , Hatice Birtane¹ ,
M. Vezir Kahraman¹ 

¹Chemistry Department, Faculty of Science, Marmara University, 34722 Istanbul, Türkiye.

²Yalova Vocational School, Department of Textile - Clothing, Shoes and Leather, Yalova University, 77200 Yalova, Türkiye.

Abstract: In our study, a selective and sensitive determination method was developed for Cu(II) ions by spectrofluorimetry. For this purpose, a polymeric membrane was prepared to determine Cu(II) ions by curing crosslinkers, functional monomers, and photoinitiators under UV light. The membrane was characterized, and the optimum conditions for determining Cu(II) ions were systematically investigated. The detection was performed at pH 5.0 in as little as 20 seconds at excitation and emission wavelengths of 376 nm and 455 nm, respectively. The linear range was $7.86 \cdot 10^{-9}$ - $1.57 \cdot 10^{-7}$ mol/L, and the method's detection limit was $2.24 \cdot 10^{-9}$ mol/L. In addition, the sensor's repeatability, stability, and life were examined, and recovery studies were conducted. As a result, the developed method has been successfully applied to wastewater samples as a real sample. In addition, determining Cu(II) ions at low concentrations can be done quickly, reliably, and with high selectivity and sensitivity.

Keywords: Cu(II) determination, fluorimetric sensor, photocuring, polymeric membrane.

Submitted: July 09, 2023. **Accepted:** December 05, 2023.

Cite this: Çubuk S, Koçoğlu N, Bayramoğlu G, Birtane H, Kahraman MV. Fluorescent Polymeric Sensor for Selective and Sensitive Detection of Cu(II) Ions in Aqueous Medium. JOTCSA. 2024; 11(1): 377-90.

DOI: <https://doi.org/10.18596/jotcsa.1324839>.

***Corresponding author. E-mail:** sonercubuk@marmara.edu.tr.

1. INTRODUCTION

With the development of industry and the increase in population, environmental pollution has become an enormous problem. Although some metal ions are essential nutrients required for various biological and physiological functions, they become toxic even at very low concentrations (1-3). Even metals such as iron, zinc, copper, and manganese may have adverse health effects when they exceed threshold concentrations (4,5). Heavy metals are considered significant environmental pollutants that enter the surroundings naturally and through human activities (6). Mainly, water and soil pollution by heavy metals is seen because of human activities such as mining, agriculture, transportation, and industrial production (7-9). When heavy metals are released into the air, water, and food, they are taken into the body directly or indirectly through inhalation, ingestion, or skin absorption (10,11).

Copper, a bio-element, is one of the most abundant heavy metals. It plays a vital role in iron absorption from the intestine, tissue maturation, formation of red blood cells, cellular respiration, electron transfer, and biological systems. It is also a cofactor in at least 30 essential enzymes (12-16). Copper is found in the oxidized Cu(II) and reduced Cu(I) states in biological systems, and their fundamental functions are dictated by their redox chemistry (17). The human body's primary sources of copper intake are seeds, grains, nuts, beans, salmon, spinach, shellfish, and beef liver (18). The Recommended Dietary Allowance (RDA) for adults over 19 years of age is 900 µg per day, while the Tolerable Upper Intake Level (UL) is 10 mg per day (19). The average copper intake from dietary sources is about 1.0 to 1.6 mg daily for adults.

The copper level in the body is maintained through the absorption of copper from the intestine and the release of copper from the liver. Therefore, as its critical side effect is cytotoxic, high copper ion levels in the body can cause liver damage (18-20). High levels of copper in the body can result in gastrointestinal symptoms such as abdominal pain, cramps, vomiting, dizziness, and diarrhea. In addition, they can lead to genetic disorders such as Menkes and Wilson's diseases (21-24). Even though the copper intake mostly depends on food, drinking water also becomes a potential source of excess exposure. The widespread use of copper, especially in agriculture, industry, and chemistry, causes contamination of the community water sources. Besides, old, corroded household pipes, plumbing fixtures, and faucets cause copper leaks and increase copper levels in tap water. The maximum copper contaminant level in drinking water has been recommended by the World Health Organization (WHO) as 20 μM (25). Even though the risk of excess intake of copper from food, water, and supplements seems to be low for adults, it is possible for children, especially those aged 1 through 8 years. Considerably high intakes, the long-term effect of excess copper intake, and the toxicity of copper are not well studied in humans.

For these reasons, it is essential to determine the copper content in environmental systems such as soil, air, water, and humans. Up to now, many methods have been established for determining Cu(II) ions. These include ion chromatography (26), surface plasmon resonance spectroscopy (SPR) (27), voltammetry (28), atomic absorption spectrophotometry (AAS) (29), inductively coupled plasma-mass spectrometry (ICP-MS) (30), UV-vis spectrophotometry (31), laser-induced fragmentation spectroscopy (LIBS) (32) and inductively coupled plasma-optical emission spectroscopy (ICP-OES) (33). Although most of the abovementioned methods provide precision, high accuracy, sensitivity, and low detection limits, they require sophisticated and expensive equipment, highly qualified personnel, and rigorous sample preparation.

Studies and significant efforts have been made to determine Cu(II) ions with short analysis time, accuracy, reliability, and low instrument costs in recent years. Many fluorescent sensors such as coumarin and derivatives (34), rhodamine (35), fluorescein (36), truxene (37), and quinoline (38) were reported and have been reported in some applications. Whether their properties (selectivity, sensitivity, response time) were improved, they all interacted with copper and formed Cu(II) complexes that resulted in distinct fluorescence responses.

In this study, we aimed to develop a new UV-curable polymeric fluorescent sensor to detect Cu(II) ions in aqueous medium. UV curing is a fast, easy, and environmentally friendly method for synthesizing polymeric membranes. These types of one-step synthesized membranes that can detect Cu(II) ions can attract attention due to their stable structure,

high efficiency and accuracy, low cost, low time consumption, and operational simplicity.

2. EXPERIMENTAL SECTION

2.1. Materials

Poly(ethylene glycol) diacrylate (PEGDA) ($M_n=575$) that contains 400-600 ppm MEHQ as an inhibitor, technical grade trimethylolpropane triacrylate (TMPTA) that contains monomethyl ether hydroquinone as an inhibitor, triphenylphosphine (TPP) (>99.0% (GC)), technical grade glycidyl trimethylammonium chloride (GTAC) that contains 2-4% chlorohydrin (>90.0% (GC)), 2-hydroxyethyl methacrylate (HEMA) (>99.0%) that contains <50 ppm monomethyl ether hydroquinone as inhibitor, N-Isopropylacrylamide (NIPAM) (>99.0%), and all other chemicals were purchased from Sigma-Aldrich and used without purification. The photoinitiator 1-hydroxy cyclohexyl-phenyl-ketone (Irgacure 184) (>99.0%) was obtained from Ciba Specialty Chemicals. In preparing the aqueous solutions, ultrapure water with a specific resistance of 18.2M Ω obtained from the Merck-Millipore Direct-Q® 3UV water purification system was used.

2.2. Instrumentations

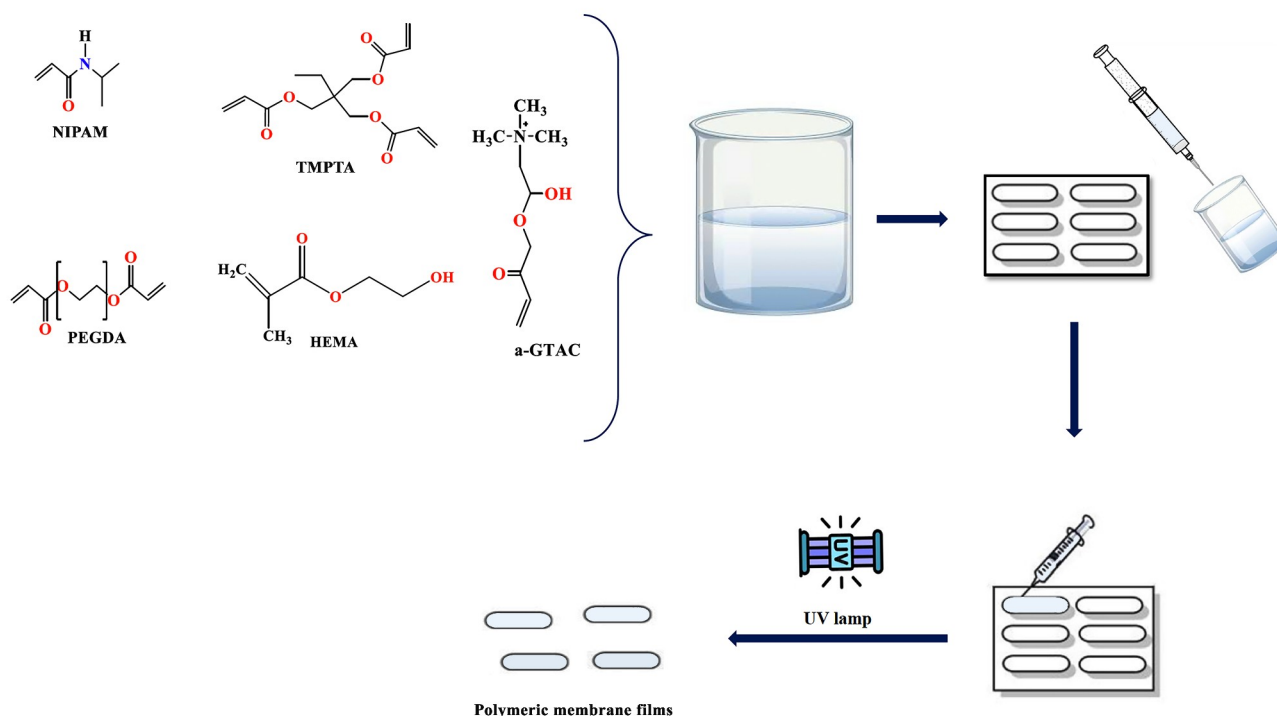
Perkin Elmer Spectrum 100 spectrometer and Philips XL30 Environmental Scanning Electron Microscope with Field Emission Gun (Equipped with EDAX-Energy Dispersive X-ray Analysis Unit) scanning electron microscope were used to obtain Fourier Transform Infrared (FT-IR) spectrum and scanning electron microscope (SEM) images of the prepared polymeric membranes, respectively. The FTIR spectrum of the solid polymeric membrane was recorded on Perkin Elmer Spectrum 100 ATR-FTIR spectrometer in the range of 4000-400 cm^{-1} at room temperature with 4 cm^{-1} resolution mode. Before SEM imaging, the membrane surfaces were coated with an approximately 300 Å thick platinum layer with Edwards S 150 B sputter coater. The Varian Cary Eclipse Fluorescence Spectrophotometer containing a 1 cm path-length quartz cuvette was used for fluorescence measurements. All pH measurements were performed using the Hanna pH-213 model pH meter.

2.3. Preparation of Polymeric Sensor

Several compositions were studied to find optimum membrane composition without fractures, cracks, and non-dispersion in the aqueous environment. First, a polymeric sensor containing aGTAC (30% wt.), HEMA (15% wt.), TMPTA (15% wt.), PEGDA (30% wt.), NIPAM (10% wt.) and photoinitiator Irgacure184 (3% of total weight) in a beaker. PEGDA was used as a binder, which provides physical and mechanical properties, and TMPTA was used as a reactive diluent, which controls the cross-linking density during polymerization. NIPAM and HEMA were used to render the membrane with environmental-sensitive properties such as swelling.

As in our previous study, the aGTAC was synthesized by reacting its oxirane groups with acrylic acid in the presence of TPP (39). The UV curing process was conducted and covered under ambient conditions. The mixture, homogenized by mixing, was poured into a Teflon® mold (12x40x 3; WxLxD, mm), covered with transparent Teflon® film to prevent the inhibiting effect of oxygen and cured

under a high-pressure UV lamp (OSRAM 300 W, λ_{\max} : 365 nm) for 3 minutes. Then, the polymeric membrane was removed from the mold. To remove unreacted monomers, obtained membranes were soaked overnight in distilled water, frozen in a freezer, and dried with a lyophilizer. The preparation of the membrane is shown in Scheme 1.



Scheme 1. The preparation of the membrane.

3. RESULTS AND DISCUSSION

3.1. Characterization

3.1.1. FTIR Analysis

The ATR-FTIR spectrum of the solid membrane is demonstrated in Figure 1. The spectrum shows a broad peak at 3352 cm^{-1} , indicating the presence of -OH groups in aGTAC and HEMA. Another peak

observed at 1707 cm^{-1} is associated with the vibration band of the -C=O group. Additionally, the spectrum shows a stretching vibration band of the C-N bond at 1449 cm^{-1} in NIPAM. Finally, the absence of a vibrational band at approximately 1634 cm^{-1} showing acrylates in the FT-IR spectrum of the membrane indicates that the cross-linked membrane was prepared successfully (39,40).

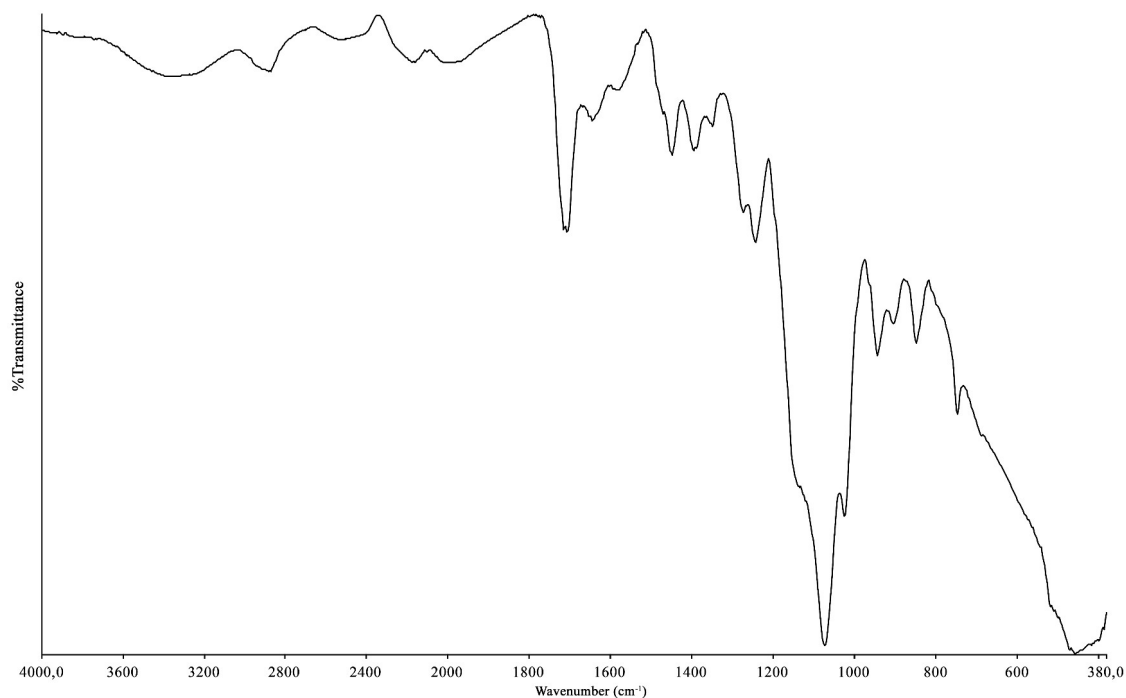


Figure 1: FTIR spectra of the membrane.

3.1.2. Surface Morphology Analysis Results

Functional groups that react with ions must be distributed uniformly throughout the polymer sensor membrane. In addition, surface homogeneity is critical for improving the polymeric membranes' sensing properties as fluorescence sensors. The

10000x magnified image of the SEM analysis performed for this purpose of the polymeric membrane is given in Figure 2. The texture shown in the SEM image in Figure 2 reveals a uniform, crack-free, and nonporous structure as desired.

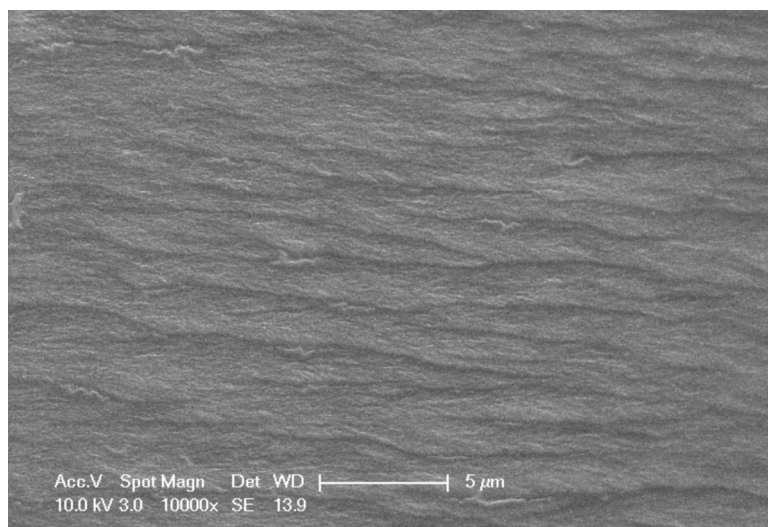


Figure 2: SEM image of the polymeric membrane at 10000X magnification.

3.1.3. Spectral characterization studies

Using fluorescent spectroscopy, the excitation and emission spectra of the polymeric membrane were recorded in the presence and absence of Cu(II) solution at a concentration of 1.57×10^{-8} mol/L. The excitation wavelength, emission wavelength, photomultiplier tube (PMT) voltage, and slit widths

were 376 nm, 455 nm, 600 V, and 10 nm, respectively. The obtained spectrum is given in Figure 3. The fluorescence intensity decreased in the presence of Cu(II) ion. It was thought to be a concurrency of static quenching in the presence of Cu(II) ions as Cu(II)- aGTAC interaction was started.

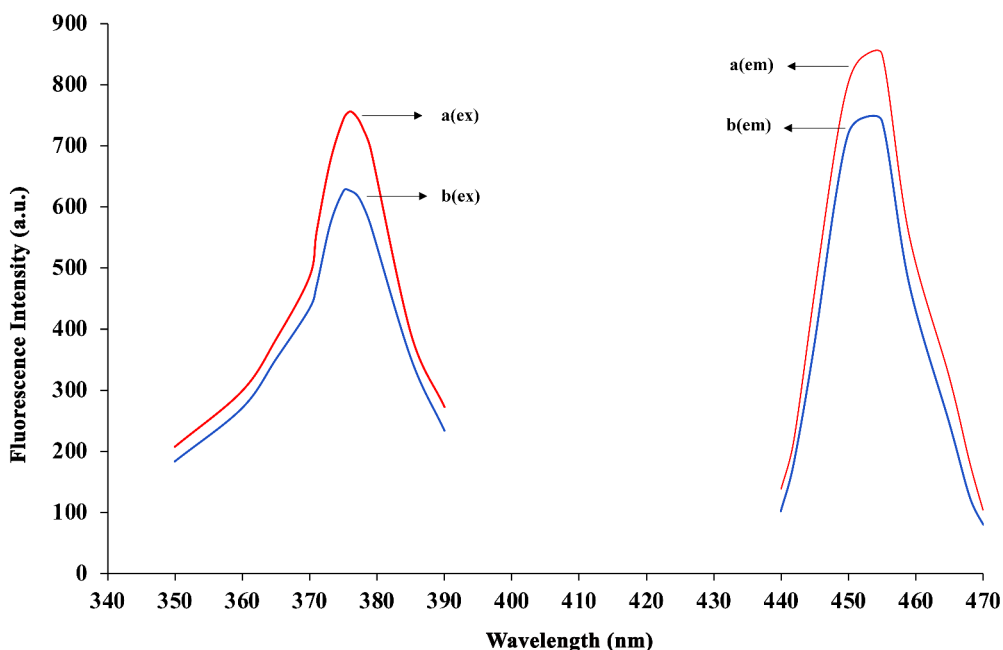


Figure 3: Excitation and fluorescence spectra of the polymeric membrane in the (a) absence (line) and the (b) presence of 1.57×10^{-8} mol/L Cu(II) ($\lambda_{\text{ex}}=376$ nm, $\lambda_{\text{em}}=455$ nm, slit widths=10 nm, photomultiplier tube voltage= 600 V).

3.1.4. Optimization of the experimental conditions

In this study, the key factor in the design of fluorescent polymeric sensors is Cu(II) recognition.

Since Cu(II)-aGTAC interaction depended on pH, fluorescence intensity could be altered between different pH ranges. Because of that, pH should be controlled to be the optimum value. To determine the pH effect on the polymeric sensor, fluorescence intensity measurements were made in the presence of 1.57×10^{-8} mol/L Cu(II) ions using buffer solutions between pH 1.0-8.0 values. The pH change trends of the fluorescence intensity of the polymeric sensor are shown in Figure 4. The fluorescence intensity slightly decreases in the range of pH 1.0-3.0, sharply increases in the range of pH 3.0-5.0, and sharply decreases after reaching the maximum level at pH 5.0. The decrease at a lower pH range can be attributed to two different mechanisms. First, the protonation of hydroxonium ions of the nitrogen atom penetrates the polymeric membrane because of its greater affinity for protons and reduced mobility of electrons of the conjugated bonds. At a higher pH range, copper hydroxide precipitation competed with Cu(II)-aGTAC interaction, and the polymeric membrane was slightly swelled to decrease the fluorescence intensity. The second one is Cu(II)-NIPAM complex formation. All the acrylic/methacrylic groups of the components react

with each other under UV light with the presence of a photoinitiator, thereby resulting in an efficiently aGTAC grafted cationized membrane along with amine and hydroxyl groups. Especially with the reaction of NIPAM and aGTMAC, the polymeric membrane results in an anionic exchanger forming both amine and quaternary amine groups. It is known that Cu(II) ions can interact with -OH groups of both aGTAC and HEMA and the amine group of NIPAM. The cross-linked structure of the polymeric membrane inhibits the interaction of the quaternary ammonium groups from aGTMAC with the amine groups of NIPAM. Since NIPAM molecules have a hydrophobic group on the backbone, they tend to swell when the NIPAM-attached membrane is treated with water. This increases chain mobility and surface area, allowing functional groups and Cu(II) attachment to interact easily.

Nevertheless, amine groups of NIPAM lead to a cationic moiety at low pH degrees. Tertiary amine groups of NIPAM protonated at a pH below 2 and positively charged NIPAM would repel Cu(II) ions like aGTMAC. Cu(II) ions induce deprotonation of -NH groups in amide bonds and lead to the formation of Cu(II) complexes (41). Considering the obtained results, pH 5.0 was chosen to conduct further experiments.

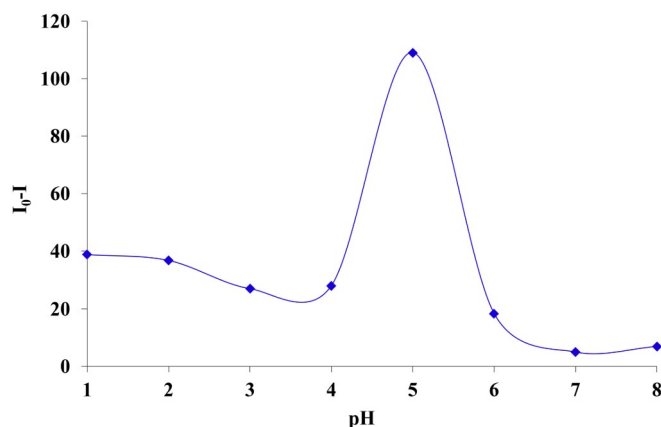


Figure 4: pH effect on fluorescence intensity ($C=1.57 \times 10^{-8}$ mol/L Cu(II)).

3.1.5. Determination of the Response Time

To determine the change in fluorescence intensity of the sensor with time, measurements were made in the presence of 1.57×10^{-8} mol/L Cu(II) ions at 5-second intervals for 200 seconds. As shown in Figure 5, the fluorescence intensity of the polymeric sensor increased with the increase of time, reached

equilibrium within 20 seconds, and did not change until 200 seconds. Since the fluorescence intensity remained constant within 20-200 seconds, the polymeric sensor could serve as a rapid and reliable probe for Cu(II) ions with the minimum 20-second waiting requirement.

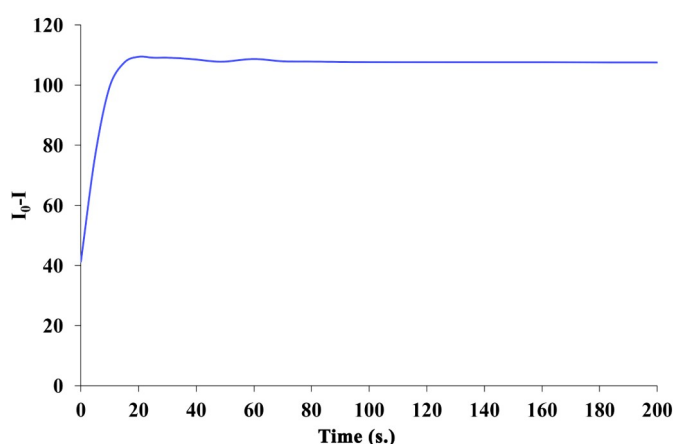


Figure 5: Effect of time on fluorescence intensity ($C=1.57 \times 10^{-8}$ mol/L Cu(II), pH=5).

3.1.6. Linear Range and Limit of Detection (LOD)

A calibration curve was established with the fluorescence intensities against the concentration of 6 samples containing Cu(II) ions within the 7.86×10^{-9} - 1.57×10^{-7} mol/L (0.5 - 10 ppb) to determine the calibration range. All samples were prepared in optimum conditions according to the experimental procedure, and fluorescence intensities were measured at 455 nm emission and 376 nm excitation wavelengths. The results indicated that increased Cu(II) ion concentration in the given range decreases the fluorescence intensity significantly. As a result, a linear plot with good linearity ($R^2=0.9954$)

was obtained to determine the slope, as shown in Figure 6.

Solutions ($n=7$) containing 7.86×10^{-9} mol/L Cu(II) were used to calculate the proposed method's detection limit. The detection limit ($LOD: 3 \times SD / m$) was calculated according to the IUPAC recommendations (42). It was found to be 2.24×10^{-9} mol/L. In this equation, SD indicates the standard deviation of 7 replicate measurements of 7.86×10^{-9} mol/L Cu(II) solution, and m shows the slope of the calibration line.

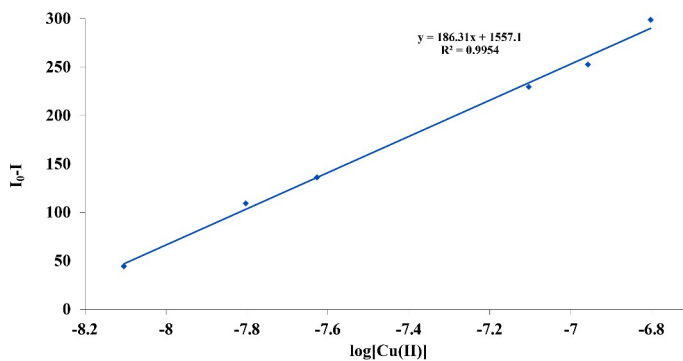


Figure 6: The calibration curve of the polymeric membrane ($\lambda_{ex}\lambda_{em}$: 376 nm/455 nm; pH:5.0; $t= 20$ s); (I_0-I) where I_0 and I are the fluorescence intensities in 7.86×10^{-9} and 1.57×10^{-7} mol L⁻¹ Cu(II), respectively.

3.1.7. Sensor Regeneration and Reusability Studies

The regeneration of the polymeric membrane was performed by a 1-minute distilled water washing followed by 30 seconds of pH 5.0 buffer solution washing. It was observed that the fluorescence intensity was found to almost fully recover after the washing process, even after 250 washing cycles.

This can be attributed to the non-affinity of the buffer solution with the polymeric membrane. One can see 30 regeneration results obtained from the regeneration process in Figure 7. The standard deviation (SD) of fluorescence intensities was calculated as ± 3.7 .

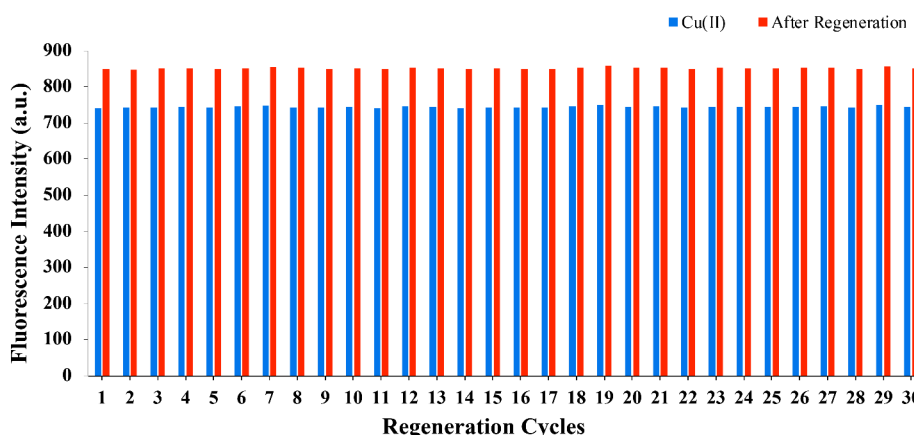


Figure 7: The effect of regeneration on fluorescence intensity of the sensor with distilled water and pH:5.0 buffer after 1.57×10^{-7} mol/L Cu(II) ion contact.

3.1.8. Reliability, Stability, and Repeatability

Reliability, stability, and repeatability are essential factors in evaluating the sensors' performance, and they play a crucial role in sensor applications. To investigate the reliability and stability of the prepared polymeric membrane sensor, it was stored in a desiccator, which was kept in the dark. The fluorescence intensity was recorded at regular intervals over six months; the results are shown in Figure 8. In line with the results in Figure 8, the change between the initial and final fluorescence intensities was only within a range of $\pm 5\%$ at the end of 6 months, which means the lifetime of the polymeric membrane is acceptable for analytical applications. To determine the short-term stability of

the polymeric membrane, it was exposed to a 1.57×10^{-8} mol/L Cu(II) solution for ten hours, and fluorescence intensity measurements were recorded at intervals of 10 min. The standard deviation of $\pm 3.4\%$ was achieved, and based on this result, it can be said that the short-term stability of the polymeric membrane is reasonable. The stability results can be ascribed to effective Cu(II)-aGTAC interaction. The repeatability of the results was also determined by using five polymeric membranes with the same formulation, and the fluorescence intensity measurements were carried out under optimum conditions according to the above-mentioned experimental procedure. A standard deviation of $\pm 2.3\%$ was achieved.

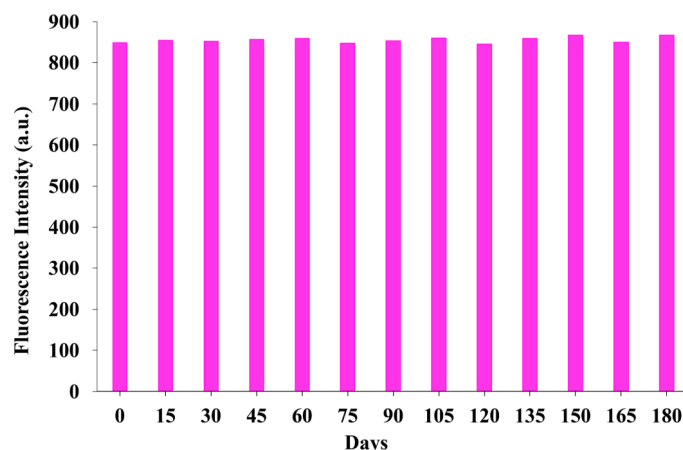


Figure 8: The fluorescence intensity changes at regular intervals during six months membrane. These results indicate satisfactory repeatability of the polymeric membrane. ($\lambda_{ex}/\lambda_{em}$: 376 nm/455 nm; pH 5.0; $t=20$ s).

3.1.9. Selectivity of Cu(II) ions toward metal ions

Selectivity is a crucial factor for a new sensor in real analytical applications. Since the interference of different ions can have a negative or positive effect on Cu(II) detection, the selectivity of the polymeric membrane to Cu(II) against other ions, including using Zn^{2+} , Fe^{3+} , Ni^{2+} , Cd^{2+} , Au^{3+} , Ag^+ , Mn^{2+} , and Hg^{2+} were investigated. To investigate the selectivity of the prepared polymeric sensor membrane against Cu(II) ions, the fluorescence intensities of 1.57×10^{-8} mol/L Cu(II) solution were measured in

the presence of 10 equivalents of each of the eight metal ion solutions. Measurements were completed by increasing the amount of coexisting ions up to the concentration where the change in fluorescence intensity was a maximum of $\pm 5\%$. The upper limit concentration values of coexisting species results are given in Table 1. As a result, it was found that the detection of Cu(II) ions could be made selectively in the presence of ions above with mole amounts that vary from 950 to 1172.

Table 1: The effect of common metal ions on determining Cu(II) under optimum conditions.

Species	x-fold higher than Cu(II) mol number	Concentration of the foreign ions (mol/L) ($mol\ L^{-1}$)
Fe(III)	1133	1.78×10^{-5}
Hg(II)	950	1.49×10^{-5}
Zn(II)	968	1.52×10^{-5}
Cd(II)	1127	1.77×10^{-5}
Mn(II)	1153	1.81×10^{-5}
Ag(I)	1172	1.84×10^{-5}
Au(III)	962	1.51×10^{-5}
Ni(II)	1083	1.70×10^{-5}

3.1.10. Analytical applications of the sensor

SPS-WW1 and SPS-WW2 certified wastewater reference (CRM) solutions diluted with pH:5 buffer solution were used to evaluate the analytical application of the polymeric membrane. The Cu(II)

ion concentrations were 6.49×10^{-6} and 3.25×10^{-5} mol/L for SPS-WW-1 and SPS-WW-2, respectively. The relative error values were calculated as 2.78% and 3.07%. The obtained results were by the certificate value (Table 2).

Table 2: Real sample analysis results with our method (n = 6).

Sample	Our Method (mol/L)	Certificate Value (mol/L)	Relative Error (%)
SPSWW-1	$(6.49 \pm 0.08) \times 10^{-6}$	$(6.30 \pm 0.01) \times 10^{-6}$	2.78
SPSWW-2	$(3.25 \pm 0.11) \times 10^{-5}$	$(3.15 \pm 0.04) \times 10^{-5}$	3.07

To evaluate the recovery performance of the polymeric membrane, tap water samples were spiked with three different concentrations of Cu(II) (1.57×10^{-8} , 4.71×10^{-8} , and 7.85×10^{-8} mol/L, respectively) were tested. No treatment was applied to it before the tap water analysis. As shown in Table 3, the recovery values of tap water samples

spiked with Cu(II) were 102.5%, 103.3%, and 104.1%, respectively.

Considering all the results obtained, one can see that the proposed method has the potential for Cu(II) determination in water samples with high accuracy.

Table 3: The application of polymeric membrane for Cu(II) detection in tap water samples (n=6).

Sample	Spiked Cu(II) (mol/L)	Our study (mol/L)	Recovery (%)
Tap water	1.57×10^{-8}	$(1.61 \pm 0.10) \times 10^{-8}$	102.5
	4.71×10^{-8}	$(4.87 \pm 0.06) \times 10^{-8}$	103.3
	7.85×10^{-8}	$(8.17 \pm 0.08) \times 10^{-8}$	104.1

3.1.11. Comparison of the proposed method with other techniques for Cu(II) determination

In Table 4, the selected methods used to determine Cu(II) and our proposed method were compared briefly, and some performance characteristics were given (43-51). As we mentioned before, atomic absorption spectroscopy (AAS), atomic emission spectrometry (AES), and inductively coupled plasma

mass spectrometry (ICP-MS) are mainly used for the determination of Cu(II) (52-54). Although the detection limits of these methods are sufficient, there are disadvantages, such as expensive and large instrumentation and extended analysis time. Nevertheless, its 20-second response time, relatively low LOD value, and high recovery rate are superior to those reported for copper ion detection.

Table 4: Comparison of selected Cu(II) detection methods.

Reference	Method	pH	LOD	Linear range	Time	Medium	Recovery
43	Voltammetric	pH:4.6	2.10^{-8} mol/L (1.29 ppb)	5.10^{-8} - $3.54.10^{-6}$ mol/L (3 - 225 ppb)	15 min.	River water, human hair	%95.97-98.22
44	Colorimetric	pH:7	$3.4.10^{-6}$ mol/L (0.22 ppm)	$3.93.10^{-6}$ - $9.4.10^{-5}$ mol/L (0.25 - 6 ppm)	5 min.	Wastewater	%93.48- 114.04
45	Spectrophotometric	pH:6	$2.5.10^{-7}$ mol/L (0.015 ppm)	$7.0.10^{-7}$ - $1.0.10^{-4}$ mol/L (0.04 - 6.35 ppm)	2 min.	Tap water, river water, lake water	%98.5-102.1
46	Spectrofluorimetric	pH:7	$3.7.10^{-8}$ mol/L (2.35 ppb)	$0.5.10^{-8}$ - 8.10^{-8} mol/L (0.31 - 5 ppb)	20 min.	Tap water, pool water,	%95-106
47	Flame Atomic Absorption Spectrophotometric (FAAS)	-	1.10^{-5} mol/L (635 ppb)	$7.9.10^{-7}$ - $7.9.10^{-5}$ mol/L (0.05 - 5 ppm)	10 min.	Oil seed samples	%95.5-102.7
48	Modified Screen Printed (MSPE; electrode VI) Potentiometric	pH:3-7	$8.8.10^{-8}$ mol/L (55.9 ppb)	$8.8.10^{-8}$ - $1.0.10^{-2}$ mol/L (5.59 -6.35.10 ⁶ ppb)	3 s.	Tap water, river water, well water	%98.67-100.61
48	Modified Gold nanoparticle Screen Printed (GNP's,SPE; electrode X) Potentiometric	pH:2-8.5	$5.3.10^{-10}$ mol/L (0.03 ppb)	$5.3.10^{-10}$ - $1.0.10^{-2}$ mol/L (0.03 -6.35.10 ⁵ ppb)	7 h.	Tap water, river water, well water	%99.78-100.2
49	Cloud Point Extraction / Spectrophotometric	pH:7	$2.2.10^{-9}$ mol/L (0.140 ppb)	3.10^{-8} - $7.9.10^{-7}$ mol/L (2 - 50 ppb)	10 min.	Lake water, fish muscle	%97-98.2
50	Cloud Point Extraction / Spectrophotometric	pH:6	$8.9.10^{-9}$ mol/L (0.57 ppb)	2.10^{-8} - $5.5.10^{-7}$ mol/L (1 - 35 ppb)	15 min.	Mineral water, sea water, lettuce, cabbage, spinach, nuts, white bread, tomatoes	%95.6-104.3
51	Inductively coupled plasma- atomic emission (ICP-AES)	pH:5-7	2.10^{-8} mol/L (1 ppb)	$3.93.10^{-9}$ - 3.10^{-8} mol/L (0.25 - 2 ppb)	300 min.	Wastewater	%98
This study	Spectrofluorimetric	pH:5	$2.24.10^{-9}$ mol/L (0.142 ppb)	$7.86.10^{-9}$ - $1.57.10^{-7}$ mol/L (0.5-10 ppb)	20 s.	Wastewater	%102.4-104.1

4. CONCLUSION

Even though aGTAC and Cu(II) were used to prepare antimicrobial systems, aGTAC for Cu(II) detection is a new approach. A new fluorescent polymeric sensor for selective and sensitive detection of Cu(II) ions in aqueous media was successfully prepared by UV curing by introducing aGTAC and NIPAM into the commercially available acrylic oligomers. UV light induces the polymerization and leads its preparation with high yields, stable structures, low energy consumption, low reaction times, lower volume of unreacted components, no need for further purification methods, and zero volatile organic components. This method allows the production of an easy and efficient polymeric sensor. Our new UV-curable polymeric fluorescent sensor with hydrophilic positively charged glycidyl trimethylammonium functionalities showed selective fluorescent quenching against Cu(II) ions with a detection limit of $2.24 \cdot 10^{-9}$ mol/L and a response time of 20 seconds.

Furthermore, the method was applied with excellent recovery results for Cu(II) ions added to real water samples. Again, selective detection of Cu(II) ions in the presence of coexisting ions with mole amounts ranging from 950 to 1172 was achieved. As a result, our method can be an alternative to existing methods as an eco-friendly approach in terms of large-scale production, practical use as a sensor, not containing organic solvents for the extraction step and analysis, and minimizing waste generation.

5. CONFLICT OF INTEREST

There are no conflicts to declare.

6. REFERENCES

1. Kiran RB, Renu S. Effect of heavy metals: An overview, *Materials Today: Proceedings*. 2022; 51(1): 880-5. Available from: [<URL>](#).
2. Marchetti C. Role of calcium channels in heavy metal toxicity. *International Scholarly Research Notices*. 2013; 2013:184360. Available from: [<URL>](#).
3. Potocki S, Rowinska-Zyrek M, Witkowska D, Pyrkosz M, Szebesczyk A, Krzywoszynska K, Kozlowski H. Metal transport and homeostasis within the human body: Toxicity associated with transport abnormalities. *Curr. Med. Chem.* 2012; 19:2738-59. Available from: [<URL>](#).
4. Cannas D, Loi E, Serra M, Firinu D, Valera P, Zavattari P. Relevance of Essential Trace Elements in Nutrition and Drinking Water for Human Health and Autoimmune Disease Risk. *Nutrients*. 2020; 12(7):2074. Available from: [<URL>](#).
5. Brindha K, Paul R, Walter J, Tan ML, Singh MK. Trace metals contamination in groundwater and implications on human health: comprehensive assessment using hydrogeochemical and geostatistical methods. *Environmental Geochemistry and Health*. 2020; 42, 3819-39. Available from: [<URL>](#).
6. Jaishankar M, Tseten T, Anbalagan N, Mathew BB, Beeregowda KN. Toxicity, mechanism and health effects of some heavy metals. *Interdisciplinary Toxicology*. 2014; 7(2):60-72. Available from: [<URL>](#).
7. Briffa J, Sinagra E, Blundell R. Heavy metal pollution in the environment and their toxicological effects on humans. *Heliyon* 2020; 6(9): e0469. Available from: [<URL>](#).
8. He ZL, Yang XE, Stoffella PJ. Trace elements in agroecosystems and impacts on the environment. *Journal of Trace Elements in Medicine and Biology*. 2005; 19(2-3):125-40. Available from: [<URL>](#).
9. Gautam PK, Gautam RK, Banerjee S et al. Heavy metals in the environment: fate, transport, toxicity and remediation technologies. Editor(s): Pathania D, *Heavy Metals: Sources, Toxicity and Remediation Techniques*, Nova Sci Publishers. 2016; 60, 101-30.
10. Jaishankar M, Tseten T, Anbalagan N, Mathew BB, Beeregowda KN. Toxicity, mechanism and health effects of some heavy metals. *Interdisciplinary Toxicology*. 2014; 7(2):60-72. Available from: [<URL>](#).
11. Tchounwou PB, Yedjou CG, Patlola AK, Sutton DJ. Heavy metal toxicity and the environment. *Molecular, Clinical and Environmental Toxicology*. 2012; 101:133-64. Available from: [<URL>](#).
12. Bost M, Houdart S, Oberli M, Kalonji E, Huneau JH, Margaritis I. Dietary copper and human health: Current evidence and unresolved issues. *Journal of Trace Elements in Medicine and Biology*. 2016; 35:107-15. Available from: [<URL>](#).
13. Feng S, Gao Q, Gao X, Jiao Y. Fluorescent sensor for copper(II) ion based on coumarin derivative and its application in cell imaging. *Elsevier Inorganic Chemistry Communications*. 2019; 102:51-6. Available from: [<URL>](#).
14. Schultze MO, Elvehjem CA, Hart EB. Studies on the copper content of the blood in nutritional anemia. *Journal of Biological Chemistry*. 1936; 116, 107-18. Available from: [<URL>](#).
15. Ramdass A, Sathish V, Babu E, Velayudham M, Thanasekaran P, Rajagopal S. Recent developments on optical and electrochemical sensing of copper (II) ion based on transition metal complexes. *Coordination Chemistry Reviews*. 2017; 343:278-307. Available from: [<URL>](#).
16. Gholivand MB; Nasrabadi MR, Ganjali MR, Salavati-Niasari M. Highly selective and sensitive copper membrane electrode based on a new synthesized Schiff base. *Talanta*. 2007; 73(3):553-60. Available from: [<URL>](#).
17. Zhu Z, McKendry R, Chavez CL Signaling in Copper Ion Homeostasis. Editor(s): Storey KB, Storey JM. Volume 1, 2000, Pages 293-300. Available from: [<URL>](#).
18. Tapiero H, Townsend DM, Tew KD. Trace elements in human physiology and pathology. *Copper. Biomedicine & Pharmacotherapy*. 2003; 57(9):386-98. Available from: [<URL>](#).
19. Institute of Medicine. Dietary Reference Intakes for Vitamin A, Vitamin K, Arsenic, Boron, Chromium, Copper, Iodine, Iron, Manganese, Molybdenum, Nickel, Silicon,

Vanadium, and Zinc. Washington, DC: The National Academies Press. 2001. Available from: [<URL>](#).

20. Gray JP, Suhali-Amacher N, Ray SD. Metals and Metal Antagonists. Editor(s): Sidhartha D. Ray, Side Effects of Drugs Annual. 2017; 39:197-208. Available from: [<URL>](#).

21. Pizarro F, Olivares M, Uauy R, Contreras P, Rebelo A, Gidi V. Acute gastrointestinal effects of graded levels of copper in drinking water. *Environmental Health Perspectives*. 1999; 107(2):117-21. Available from: [<URL>](#).

22. Taylor AA, Tsuji JS, Garry MR, McArdle ME, Goodfellow Jr WL, Adams WJ, Menzie CA. Critical Review of Exposure and Effects: Implications for Setting Regulatory Health Criteria for Ingested Copper. *Environmental Management*. 2020; 65(1):131-59. Available from: [<URL>](#).

23. Shi F, Cui S, Liu H, Pu S. A high selective fluorescent sensor for Cu²⁺ in solution and test paper strips. *Dyes and Pigments*. 2020; 173:107914. Available from: [<URL>](#).

24. Zhang X, Guo X, Yuan H, Jia X, Dai B. One-pot synthesis of a natural phenol derived fluorescence sensor for Cu(II) and Hg(II) detection. *Dyes and Pigments*. 2018; 155:100-6. Available from: [<URL>](#).

25. WHO (World Health Organization). Guidelines for drinking-water quality: fourth edition incorporating the first and second addenda. Geneva: World Health Organization; 2022. Licence: CC BY-NC-SA 3.0 IGO.

26. Ali A, Shen H, Yin X. Simultaneous determination of trace amounts of nickel, copper and mercury by liquid chromatography coupled with flow-injection on-line derivatization and preconcentration. *Anal Chim Acta*. 1998; 369(3):215-23. Available from: [<URL>](#).

27. Chen H, Jia S, Zhang J, Jang M, Chen X, Koh H, Wang Z. Sensitive detection of copper (II) ion based on conformational change of peptide by surface plasmon resonance spectroscopy. *Analytical Methods*. 2015; 20(7): 8942-6. Available from: [<URL>](#).

28. Mefteh W, Chevalier Y, Bala C, Jaffrezic-Renault N. Voltammetric Detection of Copper Ions on a Gold Electrode Modified with a N-methyl-2-naphthyl-cyclam film. *Analytical Letters*. 2018; 51(7): 971-82. Available from: [<URL>](#).

29. Şahan S, Şahin U. Determination of Copper(II) Using Atomic Absorption Spectrometry and Eriochrome Blue Black R Loaded Amberlite XAD-1180 Resin. *Clean- Soil Air Water*. 2010; 38:485-91. Available from: [<URL>](#).

30. Cao Y, Feng J, Tang L, Yu C, Mo G, Deng B. A highly efficient introduction system for single cell- ICP-MS and its application to detection of copper in single human red blood cells. *Talanta*. 2020; 206:120174. Available from: [<URL>](#).

31. Zhou F, Li C, Zhu H, Li Y. A novel method for simultaneous determination of zinc, nickel, cobalt and copper based on UV-vis spectrometry. *Optik*. 2019; 182:58-64. Available from: [<URL>](#).

32. Cao F, Jiao F, Ma S, Dong D. Laser-induced breakdown spectroscopy mediated amplification sensor for copper (II) ions detection using click chemistry. *Sensors and Actuators B: Chemical*. 2020; 371:132594. Available from: [<URL>](#).

33. Karadjov M, Velitchkova N, Veleva O, Vekichkov S, Markov P, Daskalova N. Spectral interferences in the determination of rhenium in molybdenum and copper concentrates by inductively coupled plasma optical emission spectrometry (ICP-OES). *Spectrochimica Acta Part B: Atomic Spectroscopy*. 2016; 119:76-82. Available from: [<URL>](#).

34. Feng S, Gao Q, Gao X, Yin J, Jiao Y. Fluorescent sensor for copper(II) ions based on coumarin derivative and its application in cell imaging. *Inorganic Chemistry Communications*. 2019; 102:51-6. Available from: [<URL>](#).

35. Fan J, Zhan P, Hu M, Sun W, Tang J, Wang J, Sun S, Song F, Peng X. A fluorescent ratiometric chemodosimeter for Cu²⁺ based on TBET and its application in living cells. *Organic Letters*. 2013; 15(3):492-5. Available from: [<URL>](#).

36. Jiang Y, Huang Z, Dai H, Wang L, Ying L, Kou X. A highly selective and sensitive fluorescent sensor for copper(II) ion characterized by one dichlorofluorescein moiety and two azathia-crown ether. *Asian Journal of Chemistry*. 2013; 25:8292-6. Available from: [<URL>](#).

37. Sam-ang P, Silpcharu K, Sukwattanasinitt M, Rashatasakhon P. Hydrophilic Truxene Derivative as a Fluorescent off-on Sensor for Copper (II) Ion and Phosphate Species. *Journal of Fluorescence*. 2019; 29:417-24. Available from: [<URL>](#).

38. Farhi A, Firdaus F, Saeed H, Mujeeb A, Shakir M, Owais M. A quinoline-based fluorescent probe for selective detection and real-time monitoring of copper ions- A differential colorimetric approach. *Photochemical and Photobiological Sciences*. 2019; 18:3008-15. Available from: [<URL>](#).

39. Birtane H, Şen F, Bozdağ B, Kahraman MV. Antibacterial UV-photocured acrylic coatings containing quaternary ammonium salt. *Polymer Bulletin*. 2021; 78, 3577-88. Available from: [<URL>](#).

40. Cubuk S, Taşçı N, Kahraman MV, Bayramoğlu G, Kök Yetimoglu E. Reusable fluorescent photocrosslinked polymeric sensor for determining lead ions in aqueous media. *Spectrochimica Acta Part A: Molecular and Biomolecular Spectroscopy*. 2016; 159:106-12. Available from: [<URL>](#).

41. Liu SR, Wu SP. An NBD-based Sensitive and Selective Fluorescent Sensor for Copper (II) Ion. *Journal of Fluorescence*. 2010; 21:1599-1605. Available from: [<URL>](#).

42. MacDougall D, Crummett WB et al. Guidelines for data acquisition and data quality evaluation in environmental chemistry. *Analytical Chemistry*. 1980; 52(14):2242-9. Available from: [<URL>](#).

43. Mohadesi A, Taher MA. Voltammetric determination of Cu (II) in natural waters and human hair at a meso-2, 3-dimercaptosuccinic acid self-assembled gold electrode. *Talanta*. 2007; 72(1):95-100. Available from: [<URL>](#).

44. Poesinuntakul N, Parnklang T, Sitiwed T, Chaiyo S, Kladsomboon S, Chailapakul O, Apilux A. Colorimetric assay for determination of Cu (II) ions using L-cysteine functionalized silver nanoplates. *Microchemical Journal*. 2020; 158:105101. Available from: [<URL>](#).

45. Pourbasheer E, Morsali S, Banaei A, Aghabakazadeh S, Ganjali MR, Norouzi P. Design of a novel optical sensor for determination of trace amounts of copper by UV-visible spectrophotometry in real samples. *Journal of Indus-*

trial and Engineering Chemistry. 2018; 32(3):e4110. Available from: [<URL>](#).

46. Mei L, Xiang, Y, Li N, Tong A. A new fluorescent probe of rhodamine B derivative for the detection of copper ion. *Talanta*. 2007; 72(5):1717-22. Available from: [<URL>](#).

47. Peronico VCD, Raposo JL Jr. Ultrasound-assisted extraction for the determination of Cu, Mn, Ca, and Mg in alternative oilseed crops using flame atomic absorption spectrometry. *Food Chemistry*. 2016; 196:1287-92. Available from: [<URL>](#).

48. Ali TA, Abd-Elaal AA, Mohamed GG. Screen printed ion selective electrodes based on self-assembled thiol surfactant-gold-nanoparticles for determination of Cu (II) in different water samples. *Microchemical Journal*. 2021; 160:105693. Available from: [<URL>](#).

49. Bilal M, Kazi TG, Afridi HI, Arain MB, Baig JA, Khan M, Khan N. Application of conventional and modified cloud point extraction for simultaneous enrichment of cadmium, lead and copper in lake water and fish muscles. *Journal of Industrial and Engineering Chemistry*. 2016; 40:137-44. Available from: [<URL>](#).

50. Durukan İ, Arpa Şahin A, Şatıroğlu N, Bektaş S. Determination of iron and copper in food samples by flow injection cloud point extraction flame atomic absorption

spectrometry. *Microchemical Journal*. 2011; 99(1):159-63. Available from: [<URL>](#).

51. Atanassova D, Stefanova V, Russeva E. Co-precipitative pre-concentration with sodium diethyldithiocarbamate and ICP-AES determination of Se, Cu, Pb, Zn, Fe, Co, Ni, Mn, Cr and Cd in water. *Talanta*. 1998; 47(5):1237-43. Available from: [<URL>](#).

52. Almeida JS, Souza OCCO, Teixeira LSG. Determination of Pb, Cu and Fe in ethanol fuel samples by high-resolution continuum source electrothermal atomic absorption spectrometry by exploring a combination of sequential and simultaneous strategies. *Microchemical Journal*. 2017; 137:22-6. Available from: [<URL>](#).

53. Hachmöller O, Aichler M, Schwamborn K, Lutz L, Werner M, Sperling M, Walch A, Karst U. Investigating the influence of standard staining procedures on the copper distribution and concentration in Wilson's disease liver samples by laser ablation-inductively coupled plasma-mass spectrometry. *Journal of Trace Elements in Medicine and Biology*. 2017; 44:71-5. Available from: [<URL>](#).

54. Yu J, Yang S, Lu Q, Sun D, Zheng J, Zhang X, Wang X, Yang W. Evaluation of liquid cathode glow discharge-atomic emission spectrometry for determination of copper and lead in ores samples. *Talanta*. 2017; 164(1):216-21. Available from: [<URL>](#).

